PROCEEDINGS B

rspb.royalsocietypublishing.org

Research

Cite this article: Tseng ZJ, Grohé C, Flynn JJ. 2016 A unique feeding strategy of the extinct marine mammal *Kolponomos*: convergence on sabretooths and sea otters. *Proc. R. Soc. B* **283**: 20160044.
http://dx.doi.org/10.1098/rspb.2016.0044

Received: 8 January 2016
Accepted: 9 February 2016

Subject Areas:
biomechanics, evolution, palaeontology

Keywords:
functional morphology, finite element analysis, geometric morphometrics, computed tomography, Carnivora, molluscivory

Author for correspondence:
Z. Jack Tseng
e-mail: tsengzhijie@gmail.com

Electronic supplementary material is available at http://dx.doi.org/10.1098/rspb.2016.0044 or via http://rspb.royalsocietypublishing.org.

THE ROYAL SOCIETY PUBLISHING

A unique feeding strategy of the extinct marine mammal *Kolponomos*: convergence on sabretooths and sea otters

Z. Jack Tseng[1], Camille Grohé[1] and John J. Flynn[1,2]

[1]Division of Paleontology, and [2]Richard Gilder Graduate School, American Museum of Natural History, Central Park West at 79th Street, New York, NY 10024, USA

ZJT, 0000-0001-5335-4230; CG, 0000-0002-6697-7151; JJF, 0000-0003-4705-3591

Mammalian molluscivores feed mainly by shell-crushing or suction-feeding. The extinct marine arctoid, *Kolponomos*, has been interpreted as an otter-like shell-crusher based on similar dentitions. However, neither the masticatory biomechanics of the shell-crushing adaptation nor the way *Kolponomos* may have captured hard-shelled prey have been tested. Based on mandibular symphyseal morphology shared by *Kolponomos* and sabre-toothed carnivores, we hypothesize a sabretooth-like mechanism for *Kolponomos* prey-capture, whereby the mandible functioned as an anchor. Torque generated from jaw closure and head flexion was used to dislodge prey by prying, with prey then crushed using cheek teeth. We test this hypothesized feeding sequence using phylogenetically informed biomechanical simulations and shape analyses, and find a strongly supported, shared high mandibular stiffness in simulated prey-capture bites and mandibular shape in *Kolponomos* and the sabre-toothed cat *Smilodon*. These two distantly related taxa converged on using mandibles to anchor cranial torqueing forces when prying substrate-bound prey in the former and sabre-driving forces during prey-killing in the latter. Simulated prey-crushing bites indicate that *Kolponomos* and sea otters exhibit alternative structural stiffness-bite efficiency combinations in mandibular biomechanical adaptation for shell-crushing. This unique feeding system of *Kolponomos* exemplifies a mosaic of form-function convergence relative to other Carnivora.

1. Introduction

The transition to life in a marine environment from a terrestrial one occurred at least twice in the crown clade Carnivora (the order of mammals that includes living and fossil dogs, cats, hyaenas, weasels, bears, seals, etc.)—in pinnipeds (seals, sea lions, walruses), and in otters (lutrine mustelids) [1]. Among extant marine carnivorans, the walrus (*Odobenus rosmarus*) and sea otter (*Enhydra lutris*) are particularly well adapted to feeding on hard-shelled marine invertebrates in near-shore environments. However, these two dietary specialists favour vastly different feeding strategies: walruses use suction feeding to extract the soft parts of their prey from shells, whereas sea otters pry their prey off of attached substrates using their hands and rock tools, then crush the shells with their teeth or against their chests using those tools prior to consuming the prey [2]. No other feeding mechanisms have been described for mammals consuming similar food items, and in the carnivoran fossil record, few species have remained as enigmatic in their feeding ecology and behaviour as the potentially molluscivorous mammal *Kolponomos* [3]. With two species (*K. clallamensis* and *K. newportensis*) diagnosed mostly from cranial, mandibular, and dental remains, these mammals have been reconstructed as amphibious, otter-like 'marine bears' of nearshore or littoral environments [4]. Their unique combination of osteological and dental

traits indicates that the *Kolponomos* species likely have no close living analogues for their feeding strategy.

All specimens of *Kolponomos* were recovered from Early Miocene marine deposits along the Pacific coast of Oregon, Washington, and possibly Alaska [4,5]. There is a high degree of uncertainty in the phylogenetic relationships of *Kolponomos* to other arctoid carnivorans, which has been variably placed closer to pinnipeds, ursids, or at the base of Arctoidea (see the electronic supplementary materials for additional discussion). In addition to uncertainty in phylogenetic relationships, the lifestyle of *Kolponomos* is also poorly understood, and its possible feeding strategy and dietary capabilities remain untested and unresolved. The dentition in species of *Kolponomos* superficially resembles that in living sea otters. Indeed, all dental specimens referred to *K. newportensis* exhibit extensive macroscopic wear, to the point that no enamel remains on the occlusal surface, which is made up of large 'lakes' of softer dentine surrounded by walls of enamel, as in sea otters [4]. The teeth of *K. clallamensis* are not as extremely worn, but they possess simple bunodont cusps on the cheek teeth, recalling sea otters and not the crenulated cusps typical of terrestrial omnivores such as bears (electronic supplementary material, figure S1) [4]. In this paper, we aim to analyse the feeding capability of *Kolponomos* as indicated by skull anatomy and mandibular biomechanics and shape, testing both a novel hypothesis for *Kolponomos* prey-capture and a previously proposed crushing adaptation that was never explicitly verified. Specifically, we test a novel sabretooth-like prey-capture mechanism for mollusc predation in *Kolponomos*, and the extent to which this taxon could also have been otter-like in its cheek tooth-crushing capability, together yielding a distinctive feeding sequence unlike any known extant or extinct carnivoran.

2. A unique feeding sequence in *Kolponomos*

Our proposed feeding sequence in *Kolponomos* is divided into a prying prey-capture stage and a crushing mastication stage. Several aspects of the skull anatomy of *Kolponomos* exhibit an unexpected but striking parallel with adaptations implicated in the 'canine shear-bite' model of sabretooth predatory behaviour (see the electronic supplementary material) [6,7]. We suggest that this previously unrecognized parallel is a result of the anterior part of the mandible functioning similarly as an anchor in both, the prey-capture shear-bite killing phase in sabretooths and shell-prying in *Kolponomos*. The second stage of the feeding sequence involves the previously proposed hypothesis that *Kolponomos* crushed shells with their cheek teeth as in sea otters. Below, we formulate predictions about expected mandibular biomechanics and shape in *Kolponomos* based on these two paradigms for functional convergence at the prey-capture and mastication phases (i.e. mandibular anchor and crushing cheek dentition), then test them using biomechanical finite element simulations and geometric morphometric analyses of mandibular shape.

The suite of convergent skull features common across all sabre-toothed mammals as well as sabre-toothed non-mammalian therapsids are well known, and indicative of the functional significance of those anatomical modifications [8]. Mechanically advantageous, large atlantomastoid musculature is implicated in those species by the modification of occipital morphology (see the electronic supplementary material for details). We postulate that there was an analogous emphasis on neck musculature in prey-capture in the *Kolponomos* feeding system, but instead of providing the driving force for sabretooth penetration, large atlantomastoid muscles in *Kolponomos* provided the high torque necessary to dislodge invertebrate prey tightly attached to hard substrates. The accompanying mandibular modifications for a neck-driven bite in both sabretooths (exemplified by machairodontine felids, such as *Smilodon*) and *Kolponomos* include a vertical orientation of the mandibular symphysis and deepening of the anterior part of the jaw rami (electronic supplementary material, figure S1). This characteristically deep 'chin' of derived machairodontine felid sabretooths is thought to represent an anchor, and the first point of contact during the canine shear-bite, to stabilize the masticatory apparatus for driving the elongate canines into prey [6]. In *Kolponomos*, the anterior, 'chinned' portion of the mandible would have served a similar anchoring function in prey-capture, allowing the neck muscle-driven upper incisors and canines to close around hard-shelled prey and apply a prying torque around the effective fulcrum created by the contact between the anteroventral surface of the mandible ('chin') and the substrate (figure 1). After successful prey-capture and its transport towards the posterior oral cavity (possibly via inertial feeding or tongue-assisted movement), *Kolponomos* then used broad occlusal surfaces on their cheek teeth to crush hard-shelled prey, a durophagous feeding behaviour that is analogous to the bivalve-crushing behaviour of living sea otters (a strategy complementary to tool-based bivalve- and crab-crushing in sea otters) [2,9–11].

Here, we test this proposed feeding sequence of prying and crushing in *Kolponomos*, using finite element (FE) analyses of mandibular biomechanics, geometric morphometric (GM) analyses of mandibular shape, and cheek tooth occlusal wear evidence. We compared the mandibles of *Kolponomos newportensis* with six other carnivorans, including species representing a broad phylogenetic sample and that we hypothesized to display similar feeding strategies (see Methods). Using a well-tested FE protocol for comparative functional analyses of skull structures [12], we estimated mandibular mechanical efficiency (ME; output : input force ratio), strain energy (SE; a measure of work done by the mandible during a given task, with lower energy stored indicating higher stiffness in the structure), and von Mises (VM) stress distributions (a proxy for detecting material failure under a ductile mode of deformation, as has been proposed for cortical bone [13]). Using three-dimensional GM methods, we analysed shape similarity of the symphysis and mandible among the species in our sample.

(a) Hypothesis

Based on similarities in the mandibular symphyses (broad symphyseal region with rami deeper anteriorly than posteriorly) and occipital regions (hypertrophied mastoid processes and broad occiput for increased attachment area of neck musculature) between *Kolponomos* and the sabre-toothed felid *Smilodon*, and previously tested functional morphological features of the *Smilodon* mandible [14], we hypothesize that the two carnivorans converged on using their anterior mandibles as anchors, to support shell-prying forces in the former, and sabre-driving forces in the latter. We expect to find similarly high mandibular stiffness in *Kolponomos* and *Smilodon* as is required for deformation-resisting structures, but not high ME, compared with otters and other living carnivoran species.

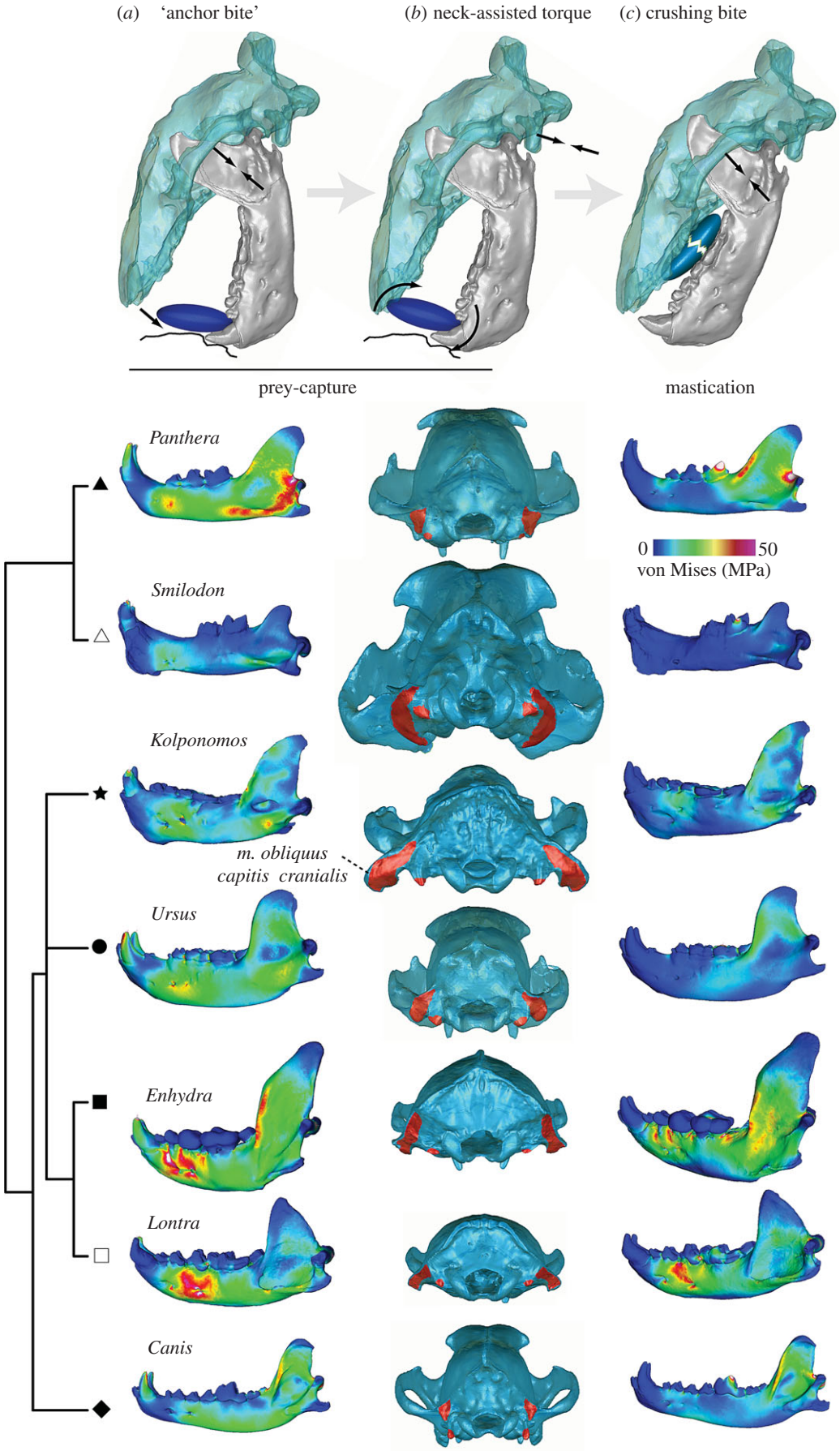

Figure 1. von Mises (VM) stress heat maps of FE simulation results and functional anatomy associated with the proposed *Kolponomos* feeding model. (*a*) 'Anchor bite' FE analyses simulated the use of lower canine teeth and the anteriorly buttressed mandible as an anchor, with corresponding VM stress distributions shown in lateral views. (*b*) Application of torque to dislodge substrate-bound hard-shelled prey by *Kolponomos* is interpreted to be facilitated by atlantomastoid musculature, with enlarged *m. obliquus capitis cranialis* attachment regions in *Smilodon* and *Kolponomos* associated with inferred anchoring bites in both taxa (skull size is standardized to common occipital condyle width). (*c*) FE analyses of unilateral crushing bite with first molar. *Kolponomos* exhibits pronounced visual differences compared with otters in both VM stress distribution and magnitude in all FE analyses. (Online version in colour.)

This result would support the reconstruction of an anchoring function for both the *Kolponomos* and *Smilodon* mandibles, for prying substrate-bound prey and in stabilizing the canine shear-bite during prey-killing, respectively. Furthermore, we expect this convergence in function to be reflected in more similar mandibular shapes between *Kolponomos* and *Smilodon* than with taxa to which they each are more closely related.

(b) Hypothesis corollary

Based on dental morphological similarities (simple bunodont cheek teeth with large and blunt cusps and heavy wear) between *Kolponomos* and shell-crushing sea otters, we predict that the two converged on biomechanically similar profiles during cheek tooth-crushing mastication. Similar cheek tooth morphology indicates similar use, and we expect to find more shared biomechanical characteristics between *Kolponomos* and the sea otter than what each shares with their closest relatives in this analysis. Given the known trade-off among carnivorans in having either high ME or high stiffness, but not both [15], and expected high mandible stiffness in *Kolponomos* based on predictions in our hypothesis, sea otters should also have high stiffness, but not high ME.

3. Material and methods

Specimens of the fossil arctoid *Kolponomos newportensis*, two lutrine mustelids (molluscivorous/piscivorous sea otter, *E. lutris*; faunivorous river otter, *Lontra canadensis*), the omnivorous brown bear (*Ursus arctos*, Ursidae), and sabre-toothed felid *Smilodon fatalis* were high-resolution micro-computed tomography (μCT)-scanned at the American Museum of Natural History, and models of the wolf (*Canis lupus*, Canidae) and leopard (*Panthera pardus*, Felidae) were taken from published data (see the electronic supplementary material, table S1 for CT parameters) [16]. Reconstructions of the X-ray images were performed using Phoenix Datos software (GE Measurement & Control, USA). Image segmentation and digital separation of the mandible from the cranium were performed using Mimics Research v. 17 (Materialise, Belgium). Surface meshes were 'cleaned' in Geomagic Studio v. 12 (Geomagic Inc., USA; see additional FE model details in electronic supplementary material, figure S2 and table S2) using semi-automatic functions to smooth the surfaces and standardize triangular element aspect ratios (maximum edge–edge ratio of 8 and edge–height ratio of 6) and quantity. Solid meshes of the mandibles of all species were generated in Strand7, v. 2.4.6. FE analysis software (G + D Computing Pty Ltd, Australia) using four-noded tetrahedral 'brick' elements. Known cranial specimens for both species of *Kolponomos* are incomplete; therefore, crania were used as references for muscle insertion (electronic supplementary material, figure S1) but not in actual FE analyses. For each species dataset, we constructed three FE models and used mean and standard error values to estimate analytical uncertainty and provide conservative 95% confidence intervals (CIs) in comparisons of simulation outputs, following the protocol of Tseng & Flynn [12]. For additional details of the model protocol, see the electronic supplementary material and [12,16].

Two sets of analyses were conducted. The first set simulated a prey-capture 'anchor bite', where jaw-closing muscles are recruited maximally bilaterally (with forces proportional to the estimated muscle attachment area), and bite points are located at the tips of both canines (see additional FE model details in the electronic supplementary material and figure S1). Output bite force at each canine tooth, measured at nodal constraints at the tip of the main cusp of each tooth, was transformed into ME by dividing output force by total input muscle force. Stored SE (in Joules) in each mandible model was also recorded, and values were adjusted using the equations in Dumont *et al.* [17] to correct for input force and model volume differences. In addition, dorsoventral displacement ratios (displacement in mm divided by mandible length) of the mandible at dorsoventral midpoint positions were measured on both rami at five sampling locations spanning the canine to last molar positions to evaluate mode of bending in a beam-like structure such as the mandibular ramus (electronic supplementary material, figure S2). In the second set of analyses ('mastication'), biomechanical profiles were constructed from individual, unilateral bite models from the canine tooth to the last molar to simulate crushing mastication bites [16]. The resulting ME and SE values were calculated as in the first analyses. In both sets of analyses, VM stresses were visualized as heat map distributions over the mandible models. Because the ratios between input force and muscle area were already standardized in our protocol, VM stress distributions could be compared directly across models without additional standardization [17].

In addition, we analysed mandibular shape similarity among the taxa using three-dimensional GM analyses. Fixed landmarks ($n = 16$) were used to capture overall mandible shape, and sliding semi-landmarks ($n = 100$) were used to capture the outline of the mandibular symphysis (electronic supplementary material, table S3 and figure S4). Semi-landmarks were first slid using a bending energy criterion prior to Procrustes superimposition of the combined fixed and semi-landmark datasets [16,18].

All values measured from the FE and GM analyses were subjected to a series of *K*-means ($K = 2$, 3, or 4) and hierarchical cluster analyses using the average-linkage method (unweighted pair group method with arithmetic mean (UPGMA)) on Euclidean distances to evaluate shape and biomechanical similarity among taxa under 'anchor bite' and crushing bite simulations, respectively. All data were standardized and centred prior to clustering. Multiscale bootstrap probabilities and cophenetic correlation coefficients were calculated on the cluster dendrograms to evaluate cluster stabilities (see the electronic supplementary material for all iterations of output data subjected to these analyses). All iterations of the FE and GM datasets were also analysed for phylogenetic signal using K*mult* [19] with four different tree topologies representing possible phylogenetic placements of *Kolponomos* (electronic supplementary material, figure S10). Each topological hypothesis was tested using both uniform branch lengths and calibrated branch lengths from compiled first appearance datums of clades represented by the taxonomic sample (electronic supplementary material).

In total, 24 individual FE models, with up to 17 different boundary condition variations for each were generated (electronic supplementary material, table S2), and a total of 312 analyses were run in Strand7 using the preconditioned conjugate gradient (PCG) solver (24 analyses for the 'anchor bite' in the seven species plus an alternative *Kolponomos* model, each with three different resolution models; 288 analyses of single-locus, unilateral crushing bite simulations for each cheek tooth position preserved on the specimens, both left and right sides, for each of the seven species and an alternative *Kolponomos* model with three different resolution models each; electronic supplementary material, table S4). Analyses were set at 10 000 iterations, after first searching for the optimum starting tree for the solution of nodal displacements as a PCG prior. The FE models in Strand7 and stereolithography (STL) formats can be downloaded from the Dryad repository (http://dx.doi.org/10.5061/dryad.184s0), and all CT data in tagged image file format (TIFF) format can be downloaded from MorphoSource (http://www.morphosource.org/index.php/Detail/ProjectDetail/Show/project_id/193).

4. Results

In 'anchor bite' simulations, *Kolponomos* exhibited the highest overall similarity to *Smilodon* (figures 1*a*, 2*a*, and 3*a*).

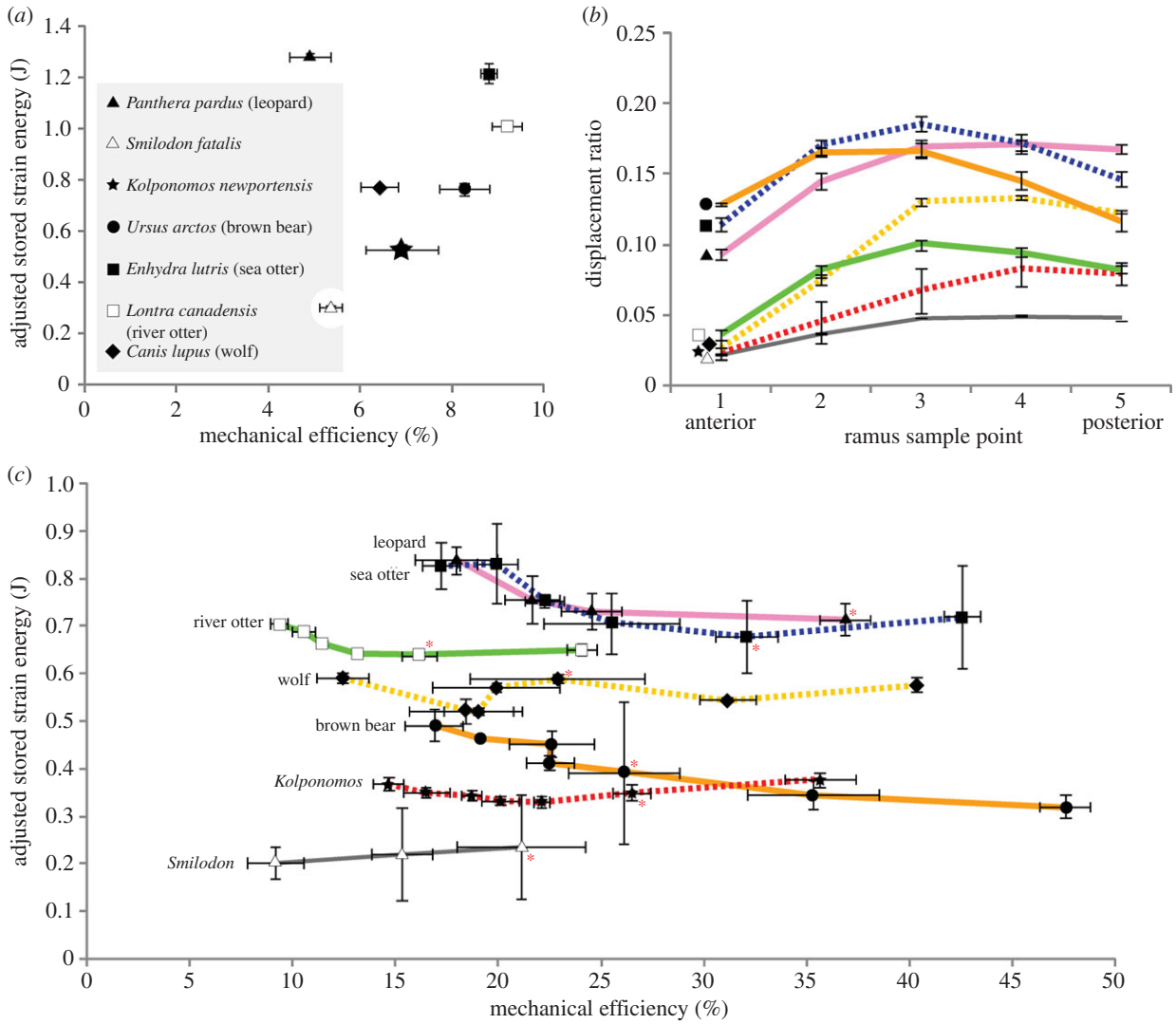

Figure 2. Results of finite element (FE) simulations of prey acquisition and mastication. (*a*) Mechanical efficiency (ME) versus adjusted stored strain energy (SE) values in 'anchor bite' prey acquisition simulations. (*b*) Dorsoventral ramal displacement ratios taken from regularly spaced sampling points along the midline of the ramus from below the canine tooth to below the end of the tooth row. (*c*) Bite profiles of ME versus adjusted stored SE of mastication FE analyses of the cheek dentition from the canine tooth to the last molar; asterisks indicate lower first molar (m1) positions. Error bars on all plots indicate 95% CIs. (Online version in colour.)

Kolponomos and *Smilodon* are most similar to each other in having low SE values (electronic supplementary material, tables S7–S9). Ramal displacement values in *Kolponomos* are intermediate between *Smilodon* and *Lontra*, and ME values of *Kolponomos* are most similar to *Canis* in being intermediate among the sampled taxa (figure 2*a*,*b* and electronic supplementary material, figure S5 and table S10). The VM stress distributions for the 'anchor bite' models show much higher stresses in the otters than in other species (figure 1*a*). The largest regions of high stress in both otter models are observed around the mandibular symphysis. In contrast, distributions of stress in the other mandibles are more evenly spread, with *Smilodon* showing the lowest overall stress, followed by *Kolponomos* (figure 1*a*).

'Anchor bite' ME values were the only results found to contain statistically significant phylogenetic signal across all four tested tree topologies for the position of *Kolponomos*, with both uniform and fossil-calibrated branch lengths (K_{mult} = 1.63–3.16, $p < 0.01$; electronic supplementary material, table S13). Correction for phylogenetic correlation using a generalized least squares approach [20] resulted in a stable cluster of the brown bear with the two otter species, and a second, less stable cluster comprising the other taxa. Combined 'anchor bite' simulation results (ME, SE, and ramal displacement) produced a dendrogram with strong support (95% approximately unbiased bootstrap probability (a.u.b.p.), 80% bootstrap probability (b.p.), cluster present in $K = 3$ and $K = 4$ of the *K*-means analyses) for the biomechanical similarity between *Kolponomos* and *Smilodon* (figure 3*a*).

FE analyses of unilateral crushing bites, biomechanical profiles or ME versus standardized SE values plotted over all tooth loci simulations, showed an overall range of 9.1–48.5% ME and 0.20–0.85 Joules of SE across the species models (figure 2*c* and electronic supplementary material, tables S4–S6). Within these ranges, the two otter species and the leopard have the highest SE (lowest stiffness) values (greater than 0.6 J), with the sea otter and leopard having the least stiff mandibles. *Smilodon* has the stiffest mandible (lowest SE value), followed by *Kolponomos* (both < 0.4 J), then the brown bear and wolf. In ME, the North American river otter and *Smilodon* have ranges lower than all other taxa; only the sea otter and brown bear exhibit ME values of the posterior cheek dentition exceeding 40% (figure 2*c* and electronic supplementary material, table S6). VM stress distributions for all single-locus bite simulations, and in particular for first molar (carnassial) simulations, show the highest stresses

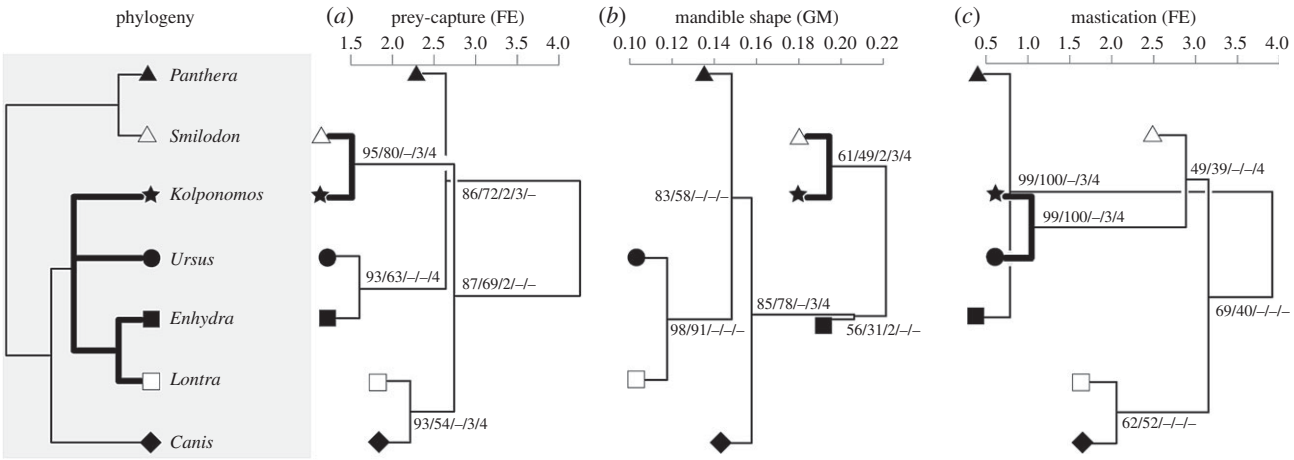

Figure 3. Hierarchical and *K*-means cluster analyses with multiscale bootstrap resampling of FE and geometric morphometrics (GM) data. (*a*) Dendrogram showing taxon clusters based on prey acquisition FE simulation results (mechanical efficiency (ME) and strain energy (SE) values from 'anchor bite' analyses, and ramus displacement). (*b*) Dendrogram showing taxon clusters based on Procrustes coordinates of mandibular fixed landmarks and symphyseal sliding semi-landmarks representing overall mandibular shape. (*c*) Dendrogram showing taxon clusters based on crushing bite mastication FE simulation results (ME and SE values from homologous tooth loci present in all taxa analysed: canine tooth, fourth premolar, first molar). All cluster analyses were conducted using Euclidean distances and average linkage; for tests of phylogenetic signal in these data, see electronic supplementary material. Nodal support values are (in order listed): approximately unbiased bootstrap probability/bootstrap probability/two-cluster *K*-means/three-cluster *K*-means/four-cluster *K*-means analyses. *Smilodon* and *Kolponomos* are most similar to each other in prey acquisition FE analysis results and overall mandible shape, whereas *Kolponomos* and *Ursus* are most similar in mastication FE analysis results.

overall in the leopard, sea otter, river otter, and wolf (all show mandibular regions with greater than 40 MPa VM stress; figure 1*c*). All others show relatively low levels of stress across the mandible (figure 1*c* and electronic supplementary material). The mandible of *Smilodon* is the least stressed in these simulations, a trend coupled with both the lowest ME and SE at all three bite positions (canine, fourth premolar, first molar; figure 2*c* and electronic supplementary material, table S6). *Kolponomos* clustered strongly with the brown bear in crushing bite simulation results (99% a.u.b.p., 100% b.p., cluster present in $K = 3$ and $K = 4$ in *K*-means analyses; figure 3*c*) and this cluster is next linked to *Smilodon*; this similarity between *Kolponomos* and the brown bear is present in all analytical iterations of the dataset (electronic supplementary material, figures S6–S8). No statistically significant phylogenetic signal was detected in these analyses (electronic supplementary material, table S13).

In overall mandible shape, *Kolponomos* and *Smilodon* are most similar to each other (figure 3*b* and electronic supplementary material, tables S11 and S12); this grouping receives strong support from *K*-means clustering ($K = 2$, 3, and 4 all show this grouping) and low support from multiscale bootstrap (61% a.u.b.p., 49% b.p.; figure 3*b* and electronic supplementary material, figure S9*a*). Low support is partly evidenced by the fact that when symphyseal semi-landmarks are analysed in isolation, *Kolponomos* and *Smilodon* cluster with each other within a larger group otherwise lacking well-defined subclusters (electronic supplementary material, figure S9*b*). *Kolponomos* and *Smilodon* are very similar in the shape of their symphyses, but are less so in other regions of the mandible (electronic supplementary material, figure S4*c*). In addition, analysis of only fixed mandibular landmarks produced a cluster of *Kolponomos* and the leopard, based on overall similarities in positions of homologous teeth (p4, m1) and posterior ramus (electronic supplementary material, figure S4*b* and figure S9*c*). The fixed mandibular landmark dataset also represents the only GM dataset among all the iterations to contain a statistically significant phylogenetic signal when a Brownian motion model of evolution is assumed ($K_{mult} = 0.76–0.82$, $p = 0.01–0.03$; electronic supplementary material, table S14). Accounting for phylogenetic correlation resulted in a cluster of *Kolponomos* with the brown bear and river otter.

5. Discussion

Bootstrapped cluster analyses of 'anchor bite' simulation data show that *Kolponomos* and *Smilodon* share similar mandibular biomechanics (particularly stiffness) and stress distributions (figure 3*a*). *Kolponomos* and *Smilodon* also are similar in mandibular shape (particularly of the symphysis; figure 3*b* and electronic supplementary material, figures S4*c* and S9*a*), both providing support for the hypothesized convergent function and structure of the mandible as an anchor in the specialized prey-capture mechanisms in each. Although distinct in inferred prey-capture behaviour, both taxa exhibit mandibular biomechanics consistent with a similar stable anterior pivot point and key functions of the anterior dentition in each, supporting a prying incisor/canine bite for *Kolponomos* and a canine shear-bite for *Smilodon* during prey-capture (figure 1). Therefore, these data support our hypothesis: *Kolponomos* and the sabretooth *Smilodon* converged on the proposed anterior anchoring function of their mandibles inferred from musculoskeletal evidence and supported by FE and GM analyses.

Unilateral crushing bite simulations across the cheek dentitions of all species show that the mandible of *Kolponomos* is much stiffer than both sea and river otters, and in this regard the *Kolponomos* jaw most closely resembles the brown bear in biomechanical characteristics. At the same time, the brown bear and *Kolponomos* both also resemble *Smilodon* in having relatively stiff mandibles in unilateral crushing bites, rather than exhibiting the combination of low stiffness and high ME observed in sea otters (figure 2*c*). Therefore, results of the unilateral crushing bite simulations reject our corollary expectation of sea otter-like crushing mandibular biomechanics for *Kolponomos*. Instead, unilateral crushing bites in

Kolponomos are accomplished via higher stiffness and lower ME, whereas sea otters exhibit crushing bites arising via lower stiffness and higher ME (figures 2*c* and 3*c* and electronic supplementary material). Previously observed trade-offs in either increasing structural stiffness or ME (but not both) of carnivoran cranial shapes indicate that biomechanical differences between sea otter and *Kolponomos* mandibles, paired with similarly bunodont dentition and heavy wear in both, may represent alternative biomechanical 'solutions' to the similar requirement of a durophagous, shell-crushing diet [15]: sea otters crush prey with emphasis on force, whereas *Kolponomos* crushed prey with emphasis on stiffness.

The simulation results, together with aspects of functional musculoskeletal anatomy, offer the basis for inferring a new and unique prey-capture–mastication feeding sequence for *Kolponomos* (figure 1). Prey-capture involved the initial anchoring and wedging of the lower incisor/canine arcade between the prey and the substrate, followed by closing of the mouth, so that the upper and lower incisors and canines bracketed the shell of the prey. Next, high torque was applied by strong atlantomastoid muscles, with the anterior face of the incisors/canines and the 'chin' serving as the effective fulcrum, dislodging the prey from the hard substrate. Corresponding grooved wear facets on the posterolateral walls of lower canines and the posteromedial walls of upper canines in *Kolponomos* are consistent with tooth contact with hard surfaces such as shells during a prying bite [4]. Finally, in crushing bites, the prey shells are crushed with an otter-like cheek dentition, but achieved via higher mandibular stiffness and lower ME than estimated in sea otters. The Early Miocene Clallam Formation and Nye Mudstone of the Pacific northwest, from which skulls of *Kolponomos* are known, contain diverse molluscan faunas that include genera of clams and mussels also found today within sea otter geographical ranges (electronic supplementary material, table S15). Therefore, *Kolponomos* and the sea otter overlap in their potential prey fauna.

Considering the biomechanical data and phylogenetic relationships together, high mandibular stiffness under unilateral crushing bites of *Kolponomos* may reflect (i) a necessary characteristic of the mandible given the high stiffness requirements of the 'anchor bite' prey-capture mechanism, (ii) an alternative biomechanical solution to a shell-crushing diet compared with sea otters and/or, (iii) either an evolutionary retention of characteristics shared with ursids or convergence on them (figures 1 and 3), depending on the phylogenetic framework used (electronic supplementary material, figure S10). Future advances in both constraining the phylogenetic relationships of *Kolponomos* and better understanding its skull functional morphology will permit additional tests of these possibilities. We also note that the structural biomechanical data analysed herein does not preclude suction-feeding during prey-capture by *Kolponomos*, which may have been possible given observed convergence in suction-feeding adaptations in many different clades of marine vertebrates [3,21]. Such capability would only lend credence to a highly mosaic and complex feeding system worthy of further investigation. Additionally, comparative bone and enamel carbon and nitrogen isotope analysis as well as enamel microstructure analysis would also provide additional lines of evidence with which to reconstruct the feeding preference of *Kolponomos*.

The enlarged and anteroventrally extended mastoid processes in *Kolponomos* (expanded to the point of projecting anteriorly to the postglenoid process in lateral view) provided large areas for the attachment of the *m. obliquus capitis cranialis* as in *Smilodon*, and both taxa have mastoid processes that extend ventrally past the atlantooccipital joint, providing added leverage and torque for head flexion (electronic supplementary material, figure S3) [22]. However, in addition to anteroventral placement, the mastoid processes in *Kolponomos* also extend farther laterally than in other carnivorans examined, increasing the leverage and torque for head-turning movements controlled by the atlantomastoid muscles. Furthermore, the deeply excavated, highly rugose, and dorsoventrally elongated occipital bone in *Smilodon* and *Kolponomos* relative to other carnivorans indicates longer dorsal lever arms for the *m. rectis capitis*, which works to extend the head (electronic supplementary material, figure S3) [23]. Consequently, the neural spine of the axis, from which part of the *m. rectis capitis dorsalis major* originate, is also relatively larger in *Kolponomos* than in sea otters [4] or the other carnivorans analysed. These anatomical differences indicate that *Kolponomos* may have had both powerful head-flexing and head-lifting movements, suggesting the possibility of 'anchor bites' powered by raising the head forcefully. Therefore, head-lifting could represent an alternative or complementary strategy to the proposed mandible-anchored, head-flexing prying motion for prey-capture (figure 1). In addition to *Kolponomos*, future advances in understanding similar types of semi-aquatic feeding adaptations in fossil mammals can also be aided by comparative analyses of other taxa such as the extinct walrus *Gomphotaria*, which has also been hypothesized to be adapted for similar feeding strategies [4].

6. Summary and conclusions

Based on the anteroventrally extended and hypertrophied mastoid processes and vertically oriented and deepened mandibular symphyses shared by sabre-toothed mammals and *Kolponomos*, combined with the sea otter-like cheek tooth morphology in *Kolponomos*, we proposed and tested a unique prey-capture–mastication sequence in the feeding apparatus of this extinct marine arctoid carnivoran. This distinctive feeding sequence involved first using the mandible as an anchor for torque application, created by powerful neck musculature acting through the cranium, to dislodge hard-shelled invertebrates attached to rocky substrates. FE simulation and GM results test, and support, this model by demonstrating extensive similarities between *Kolponomos* and *Smilodon* in high mandibular stiffness during prey-capture simulations and in mandibular shape, and their distinctions from more closely related caniform (otters, wolf, and brown bear) or feliform (leopard) carnivorans, respectively. The findings support our interpretation of the anterior portion of the jaw as a functional anchoring fulcrum in both *Kolponomos* and *Smilodon* during prey-capture, for prying in the former and stabilizing the canine shear-bite in the latter.

In addition, FE analyses show that, even if the mandible of *Kolponomos* shares similar dental morphology and heavy occlusal wear patterns with the sea otter, they do not share similarly stiff mandibles in unilateral crushing bite simulations. Instead, *Kolponomos* exhibits high stiffness and low efficiency, whereas sea otters exhibit lower stiffness and higher efficiency. The much stiffer mandible in *Kolponomos* resembles bears (and *Smilodon*, to a lesser extent) and is unlike otters or the other

sampled carnivorans, and may indicate shell-crushing adaptation via a different combination of mandibular stiffness-efficiency, representing a trade-off in these biomechanical attributes compared with extant sea otters. Taken together, these data support a unique feeding repertoire in *Kolponomos* that does not have a close analogue in species in modern ecosystems. They also highlight how prey-capture strategies across vastly different environments and taxa nevertheless may be based on fundamentally similar biomechanical requirements for mandibular function, as in the marine molluscivore *Kolponomos* and hypercarnivorous terrestrial sabretooth predators such as *Smilodon*. Lastly, these findings also demonstrate a mosaic functional convergence in the mandible of *Kolponomos* within the prey-capture–mastication sequence: an initial phase of prey-capture resembling the canine shear-bite model of sabretooths, and sea otter-like dental wear and morphology but with structural stiffness emphasized over ME.

Data accessibility. FE models and stereolithography files from this study are deposited at the Dryad repository (http://dx.doi.org/10.5061/dryad.184s0). Original CT scan data from this study are deposited at MorphoSource (http://www.morphosource.org/index.php/Detail/ProjectDetail/Show/project_id/193).

Authors' contributions. Z.J.T. designed the study, collected CT data, carried out the finite element analyses, analysed data, and drafted the figures. C.G. designed the study, collected CT and laser scan data, and conducted the geometric morphometric analyses. J.J.F. contributed to the design of the study and analyses. All authors contributed to writing the manuscript, and gave final approval for publication.

Competing interests. We declare we have no competing interests.

Funding. Research was supported by the National Science Foundation (U.S.) DEB-#1257572 (to Z.J.T., C.G., J.J.F.) and Frick Postdoctoral Fellowships, Division of Paleontology, American Museum of Natural History (to Z.J.T., C.G.).

Acknowledgements. We dedicate this paper to the late Chester Tarka (AMNH), who helped photograph and illustrate the holotype skull of *Kolponomos newportensis* 30 years ago. We thank H. Towbin and M. Hill (AMNH MIF) for their assistance in CT-scanning the specimens used in this study. J. Dines (LACM) and E. Westwig and N. Duncan (AMNH) provided loans of the extant species specimens for study. N. Pyenson and D. Bohaska (NMNH) supported a loan of *Kolponomos newportensis*. W. Harcourt-Smith (AMNH/CUNY) provided access to a three-dimensional laser scanner for digitizing a lower jaw of *Amphicynodon* and N. Webb (CUNY) assisted with the scan. B. Beatty, an anonymous referee, and editor R. Mehta provided highly constructive comments that improved an earlier version of the paper.

References

1. Nowak RM. 1999 *Walker's carnivores of the world*, 313. Baltimore, MD: The Johns Hopkins University Press.
2. Ewer RF. 1973 *The carnivores*, 494. Ithaca, NY: Cornell University Press.
3. Berta A, Sumich JL, Kovacs KM. 2015 *Marine mammals: evolutionary biology*, 738. Waltham, MA: Academic Press.
4. Tedford RH, Barnes LG, Ray CE. 1994 The early Miocene littoral ursoid carnivoran *Kolponomos*: systematics and mode of life. In *Contributions in marine mammal paleontology honoring Frank C. Whitmore Jr.* (eds A Berta, TA Demere), pp. 11–32. San Diego, CA: Proceedings of the San Diego Society of Natural History.
5. Jacobs LL, Fiorillo AR, Nishida Y. 2009 Mid-cenozoic marine mammals from Alaska. In *Papers on geology, vertebrate paleontology, and biostratigraphy in Honor of Michael O. Woodburne* (ed. LB Albright III), pp. 171–184. Flagstaff, AZ: Museum of Northern Arizona Bulletin.
6. Akersten WA. 1985 Canine function in *Smilodon* (Mammalia; Felidae; Machairodontinae). *Contrib. Sci.* **356**, 1–22.
7. Turner A, Antón M, Salesa MJ, Morales J. 2011 Changing ideas about the evolution and functional morphology of Machairodontine felids. *Estudios Geologicos* **67**, 255–276. (doi:10.3989/egeol.40590.188)
8. Antón M. 2014 *Sabertooth*, 268. Bloomington, IN: Indiana University Press.
9. Estes JA. 1980 *Enhydra lutris*. *Mammal. Species* **133**, 1–8. (doi:10.2307/3503844)
10. Hall KR, Schaller GB. 1964 Tool using behavior of the California sea otter. *J. Mammal.* **45**, 287–298. (doi:10.2307/1376994)
11. Calkins DG. 1978 Feeding behavior and major prey species of the sea otter, *Enhydra lutris*, in Montague Strait, Prince William Sound, Alaska. *Fishery Bull.* **76**, 125–131.
12. Tseng ZJ, Flynn JJ. 2015 Convergence analysis of a finite element skull model of *Herpestes javanicus* (Carnivora, Mammalia): implications for robust comparative inferences of biomechanical function. *J. Theor. Biol.* **365**, 112–148. (doi:10.1016/j.jtbi.2014.10.002)
13. Nalla RK, Kinney JH, Ritchie RO. 2003 Mechanistic failure criteria for the failure of human cortical bone. *Nat. Mater.* **2**, 164–168. (doi:10.1038/nmat832)
14. McHenry C, Wroe S, Clausen PD, Moreno K, Cunningham E. 2007 Supermodeled sabercat, predatory behavior in *Smilodon fatalis* revealed by high-resolution 3D computer simulation. *Proc. Natl Acad. Sci. USA* **104**, 16 010–16 015. (doi:10.1073/pnas.0706086104)
15. Tseng ZJ. 2013 Testing adaptive hypotheses of convergence with functional landscapes: a case study of bone-cracking hypercarnivores. *PLoS ONE* **8**, e65305. (doi:10.1371/journal.pone.0065305)
16. Tseng ZJ, Flynn JJ. 2015 Are cranial biomechanical simulation data linked to known diets in extant taxa? A method for applying diet-biomechanics linkage models to infer feeding capability of extinct species. *PLoS ONE* **10**, e0124020. (doi:10.1371/journal.pone.0124020)
17. Dumont ER, Grosse I, Slater GJ. 2009 Requirements for comparing the performance of finite element models of biological structures. *J. Theor. Biol.* **256**, 96–103. (doi:10.1016/j.jtbi.2008.08.017)
18. Grohé C, Tseng Z, Lebrun R, Boistel R, Flynn JJ. 2015 Bony labyrinth shape variation in extant Carnivora: a case study of Musteloidea. *J. Anat.* (doi:10.1111/joa.12421)
19. Adams DC. 2014 A method for assessing phylogenetic least squares models for shape and other high-dimensional multivariate data. *Evolution* **68**, 2675–2688. (doi:10.1111/evo.12463)
20. Garland Jr T, Ives AR. 2000 Using the past to predict the present: confidence intervals for regression equations in phylogenetic comparative methods. *Am. Nat.* **155**, 346–364. (doi:10.1086/303327)
21. Ferry-Graham LA, Lauder GV. 2001 Aquatic prey capture in ray-finned fishes: a century of progress and new directions. *J. Morphol.* **248**, 99–119. (doi:10.1002/jmor.1023)
22. Antón M, Salesa MJ, Pastor JF, Sanchez IM, Fraile S, Morales J. 2004 Implications of the mastoid anatomy of larger extant felids for the evolution and predatory behaviour of sabretoothed cats (Mammalia, Carnivora, Felidae). *Zool. J. Linn. Soc.* **140**, 207–221. (doi:10.1111/j.1096-3642.2003.00093.x)
23. Davis DD. 1964 The giant panda: a morphological study of evolutionary mechanisms. *Fieldiana: Zool. Mem.* **3**, 1–339.